



Fine control of critical dimension for the fabrication of large bandgap high frequency photonic and phononic crystals

J. Cuffe^{a,b,*}, D. Dudek^b, N. Kehagias^b, P.-O. Chapuis^b, V. Reboud^b, F. Alsina^b, J.G. McInerney^a, C.M. Sotomayor Torres^{b,c}

^a Tyndall National Institute, University College Cork, Cork, Ireland

^b Catalan Institute of Nanotechnology, CIN2 (ICN-CSIC), Campus de la UAB 08193 Bellaterra (Barcelona), Spain

^c ICREA, Institució Catalana de Recerca i Estudis Avançats, 08010 Barcelona, Spain

ARTICLE INFO

Article history:

Received 19 September 2010

Accepted 17 December 2010

Available online 24 December 2010

Keywords:

Photonic crystal

Phononic crystal

PhoXonic crystal

Electron beam lithography

Reactive ion etching

ABSTRACT

In this work artificial crystal structures designed to exhibit large and simultaneous photonic and phononic bandgaps, known as phoXonic crystals, are fabricated in silicon. Simulations have shown that honeycomb and square symmetry phoXonic crystals with high filling-fractions can produce large bandgaps in the photonic and phononic dispersion relations. To achieve this at hypersonic phononic frequencies and infrared (telecommunications) photonic frequencies, critical dimensions smaller than 100 nm are typically required. In this paper, dose variation for Electron Beam Lithography (EBL) combined with Reactive Ion Etching (RIE) and Thermal Oxidation (TO) are shown to be effective methods to carefully control these parameters.

© 2011 Elsevier B.V. All rights reserved.

1. Introduction

Periodically structured materials capable of simultaneously influencing photon and phonon propagation on the nanoscale, sometimes referred to as phoXonic crystals, offer the opportunity to tailor photon–phonon interactions, releasing a realm of rich physics and potentially leading to novel opto-acoustic devices [1].

With an appropriate choice of materials and geometry of the patterned crystal, it is possible to fabricate a structure that simultaneously exhibits a photonic and phononic bandgap. Monocrystalline silicon is an appropriate choice of material for the fabrication of crystals that exhibit infrared photonic bandgaps and hypersonic phononic bandgaps, as it exhibits both a large optical and acoustical contrast with air. Moreover, as the fabrication process can be performed with the standard CMOS machining tools, it is a suitable material for very large scale integration (VLSI). While much research has been performed on photonic crystals ranging from the infrared to the visible, to date, the majority of the experimental research on phononic crystals has been in the ultrasonic regime (100's of MHz) or below [2]. Hypersonic (>1 GHz) phononic crystals have previously been achieved in materials such as polymers [3] and self-assembled silica and polystyrene beads [4,5] using interference lithography and vertical deposition self

assembly, respectively. There are, however, no reports of silicon phononic crystals operating at hypersonic frequencies.

The realization of these devices operating at hypersonic acoustic frequencies and infrared photonic frequencies (telecommunications wavelengths) is challenging, as the minimum feature sizes of the crystal structure lie in the range of tens of nanometers. The scale invariant nature of the wave equations means that the mid-gap frequency scales approximately inversely with the periodicity of the lattice; thus, higher midgap frequencies appear at smaller lattice constants. It has also been shown that the width of the bandgap for solid-air phoXonic crystals increases with the filling fraction [6], which is a measure of the size of the air inclusion in relation to the solid host material. The increase in filling fraction results in a decrease of the critical dimension, which is given by $d_{\text{critical}} = a - 2r$ where a is the lattice constant of the crystal structure and r is the radius of the inclusions.

In this paper, we succeed in the fabrication of phoXonic crystal structures in silicon with critical dimensions down to 20 nm, which FDTD simulations have predicted to exhibit large, high frequency simultaneous photonic and phononic bandgaps [6].

2. Design

The formation of photonic and phononic bandgaps depends primarily on three parameter sets: the acoustic and dielectric constants of host and inclusion materials, the crystal symmetry and the filling fraction. Both square and honeycomb geometries were

* Corresponding author at: Tyndall National Institute, University College Cork, Cork, Ireland.

E-mail address: john.cuffe@icn.cat (J. Cuffe).

investigated for pitch of 500 nm and radius-to-pitch (r/a) ratios ranging from 0.32 to 0.48. This corresponds to filling fractions ranging from 0.32 to 0.72 for a square lattice (f.f. = $\pi r^2/a^2$), and from 0.74 to 1.67 for a honeycomb (Suzuki Phase) lattice (f.f. = $4\pi r^2/\sqrt{3}a^2$). These designs are predicted to exhibit bandgaps in the frequency range [2.8;7.13] GHz for hypersonic phonons and [239;288] THz for infrared photons [6]. As well as potential important applications for THz photonics and telecommunications, these structures also exhibit midgap frequencies in a range commensurate with detection by the inelastic light scattering technique of Brillouin Light Scattering (BLS) spectroscopy, which can be used to measure directly the acoustic phonon dispersion relation [4].

3. Fabrication

The phoXonic crystal structures were fabricated with (100) silicon wafers, Boron doped with a resistivity of 20–40 Ωcm . To pattern the simulated structures, high resolution EBL was employed, using a RAITH GmbH 150 TWO lithography system. The polymer was a 495 k PMMA resist from MicroChem Corp. As the resist thickness is a critical parameter in the subsequent RIE step, two different PMMA layer thicknesses of 150 and 250 nm were compared, obtained by spincoating on 20×20 mm silicon samples at 1000 and 4000 rpm, respectively. This layer thickness range was chosen taking into consideration Monte-Carlo simulations of the electron beam scattering in PMMA layers. The exposure was carried out with an acceleration voltage of 10 kV and an initial area dose of $80 \mu\text{C}/\text{cm}^2$. The optimum step-size for the exposure was also investigated and found to be 10 nm. This method was compared to the exposure of phoXonic crystal designs in which the hole diameter is pre-defined and the exposure executed at a constant dose.

After development and post-baking for 60 s at 100°C , the pattern transfer from the exposed PMMA mask into silicon substrate was carried out using an Inductively Coupled Plasma (ICP) ALCA-TEL 601E RIE reactor. Initial parameters for the etching procedure were estimated from simulations that solved the drift and diffusion equations for charged particles, in which the electron density and ion distribution were calculated as a function of input power and gas pressure, described elsewhere [7]. The etching parameters were further refined by adjusting rf-power, bias voltage, chamber pressure, O_2 , SF_6 and C_4F_8 gas flows and the etching time. To obtain high aspect ratios, while simultaneously achieving defect-free side walls, the bias voltage and the rf-power were optimized while the other parameters were kept constant. Each etching procedure was stopped before the remaining polymer etch mask completely disappeared, to protect the surface of the sample. Finally, each sample was treated in a high-pressure oxygen-plasma to remove organic contamination from the sample surface.

After the RIE procedure, a dry thermal oxidation was performed in a high temperature oven in an oxygen atmosphere. Thermal oxidation is a slow growing process based on the diffusion of oxygen molecules onto the silicon surface which react to form silicon dioxide. The thermal silicon oxide was removed by a HF acid solution. In this way, we show that it is possible to fine tune the filling fraction of the fabricated structures. The temperature for the oxidation was set to 1000°C and the treatment time was set to 10 and 25 min for two different samples of the same structure. Taking into account the different oxidation velocities that depend on the crystal orientation, it is also thought that this may also lead to an improvement of the surface roughness.

4. Results

The fabricated structures were characterized with a LEO1530 Scanning Electron Microscope (SEM), for both top-view and

cross-section of the crystals. The broadening of the electron beam inside the polymer at higher dose leads to a progressively larger round hole shape and results in a higher quality of the structure compared with structures for which the diameter is increased directly in the design. A significant distortion of the circular hole-shape was found after EBL exposure for the thicker 250 nm PMMA film, as seen in Fig. 1(a). This effect was less apparent in the 150 nm thin layer, in which good pattern fidelity and sharp edges were conserved. The r/a -ratio was controlled from 0.27 to 0.47 by increasing the exposure dose from 80 to $168 \mu\text{C}/\text{cm}^2$. However, exposure dose values smaller than $100 \mu\text{C}/\text{cm}^2$ lead to an underexposure of the holes and residual polymer, while dose values of $168 \mu\text{C}/\text{cm}^2$ or higher resulted in a slight distortion of the round shape of the holes, until breaking of the thin residual polymer separating two holes was observed. An undercut of the polymer walls at these doses was also observed, as a result of the increased proximity effect. SEM cross-sections images of the polymer layer showed the optimum exposure dose to be $144 \mu\text{C}/\text{cm}^2$, with rectangle side walls of the polymer separating the two holes. However, the r/a -ratio at this dose is 0.39, which is lower than the desired values for the structure to exhibit large simultaneous band gaps. The distortion of the circular hole-shape was also concluded to be a direct effect of electron proximity inside the PMMA layer, as the holes at the boundary of the phononic crystal maintained a circular shape.

Comparison of the measurements of the hole-diameter taken from the SEM micrographs before and after RIE (Fig. 1b) show that the value for over-etching ranges from 12% for a filling fraction of 0.39 up to 22% for a filling fraction of 0.48. Remarkably, the critical dimensions were measured to have values in the range from 100 nm down to 22 nm for the honeycomb structures, and from 100 to 35 nm for the square lattice. This result implies that the r/a -ratio can be controlled from 0.4 up to 0.48 and 0.47, respectively. These results match well with the requirements predicted by Ref. [6] for large, high frequency photonic and phononic bandgaps. At higher r/a -ratios, the PMMA mask is over-etched and the silicon walls between holes become damaged.

The etched structures were also examined in cross-section with SEM, as shown in Fig. 2(a). It is important to note that the circular cylinders are not exactly rectangular in profile as the etching has a certain isotropy depending on the chemical reactions by the electronegative fluorine radicals. As the consequence, the thin silicon

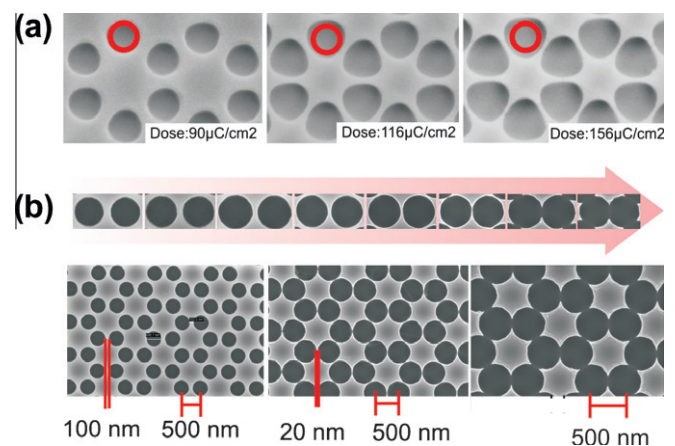


Fig. 1. (a) Top-view SEM images of 250 nm thick PMMA resist after EBL exposure and development of the honeycomb lattice. Distortion of the pattern is seen at higher doses due to the enhanced proximity of the exposures. (b) Top-view SEM images of silicon RIE-etched honeycomb lattice structures patterned using the 150 nm polymer resist. The arrow indicates increasing r/a -ratio for two holes of the unit cell etched into silicon.

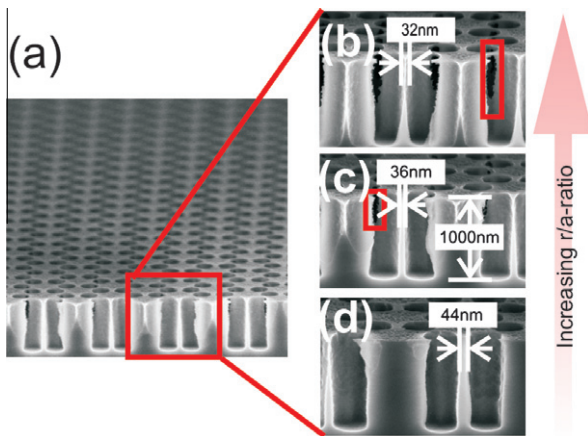


Fig. 2. (a) SEM cross-section view of the honeycomb lattice phononic crystal. (b–d) Detailed view on the cylindrical air holes in silicon for decreasing r/a -ratios with red boxes indicating the defect in the depth of the silicon walls. (For interpretation of the references to colour in this figure legend, the reader is referred to the web version of this article.)

walls show some defects in the depth as indicated by the red boxes in Fig. 2(b) and (c). These defects are invisible from top-view SEM micrographs, and show the importance of performing cross-section analysis. The structure where no damage in the silicon walls appears is shown in Fig. 2(d) has a slightly lower r/a -ratio with a value of 0.46. Nevertheless, the aspect ratio is high with a value of 22:1 measuring the etch depth of 1000 nm of the air cylinders. This result is important when measuring the phononic band-gap with Brillouin light scattering spectroscopy, taking into account the penetration depth of the light, and the formation of the phononic bandgap.

To further refine the fabricated geometry, thermal oxidation was applied as a method to achieve fine control of the filling fraction. The principle behind this method is that, due to the slow rate of oxidation of silicon, the thickness of the silicon oxide layer growth can be controlled with nanometer precision. To demonstrate the effectiveness of this method, a square lattice with the lower r/a -ratio of 0.38 was chosen for the characterization of two different oxidation steps. The initial silicon side wall thickness of 115 nm was reduced to 60 nm after 10 min of oxidation, and further reduced to 33 nm after 20 min of oxidation. As well as an increase in the r/a -ratio with increasing oxidation time, a decrease in surface and sidewall roughness is expected, though this cannot as yet be confirmed.

5. Conclusion

In this paper we succeeded in fabricating silicon phoXonic crystals, designed to give large, simultaneous bandgaps for photons at telecommunication wavelengths and phonons in the hypersonic frequency range. To achieve this we optimized the EBL and RIE parameters, to fabricate square and honeycomb lattices with lattice constants of 500 nm, and r/a -ratios ranging from 0.27 to 0.48, avoiding pattern distortions due to increasing proximity effects. The aspect ratio after the RIE procedure was remarkably high in some cases, with a value of 22:1. These structures have corresponding critical dimensions ranging from 250 nm to less than 20 nm, which is near the technological limit of a standard lithography system. We show that a limit is imposed on the thickness of the PMMA resist layer due to increased proximity effect in thicker films, which leads to a distortion of the shape of the exposed pattern. It was also demonstrated that further optimization of the filling fraction can be achieved through thermal oxidation, and work is ongoing in this regard. The following work includes the characterization of these structures, to demonstrate the predicted infrared and hypersonic photonic and phononic bandgaps.

Acknowledgement

J.C. would like to gratefully acknowledge financial support under an Irish Research Council for Science, Engineering, and Technology (ICRSET) scholarship. The authors are grateful for financial support from the FP7 projects ICT_FET TAILPHOX (Grant No. 233883), ICT_IP NANOPACK (Grant No. 216176) and the MICINN project ACPHIN (FIS2009-10150).

References

- [1] M. Eichenfield, J. Chan, R.M. Camacho, K.J. Vahala, O. Painter, *Nature* 462 (2009) 78–82.
- [2] S. Benchabane, A. Khelif, J.-Y. Rauch, L. Robert, V. Laude, *Phys. Rev. E* 73 (6) (2006) 065601.
- [3] T. Gorishnyy, J.-H. Jang, C. Koh, E.L. Thomas, *Appl. Phys. Lett.* 91 (12) (2007) 121915.
- [4] W. Cheng, J. Wang, U. Jonas, G. Fytas, N. Stefanou, *Nat. Mater.* 5 (10) (2006) 830–836.
- [5] T. Still, W. Cheng, M. Retsch, U. Jonas, G. Fytas, *J. Phys.: Condens. Matter* 20 (40) (2008) 404203–404209.
- [6] Y. Pennec, B.D. Rouhani, E.H.E. Boudouti, C. Li, Y.E. Hassouani, J.O. Vasseur, N. Papanikolaou, S. Benchabane, V. Laude, A. Martinez, *Opt. Express* 18 (13) (2010) 14301–14310.
- [7] A.V. Vasenkov, X. Li, G.S. Oehrlein, M.J. Kushner, *J. Vac. Sci. Technol. A: Vac. Surf. Films* 22 (2004) 511.